World Journal of Engineering Research
Print ISSN: 2959-9865
Online ISSN: 2959-9873
DOI: https://doi.org/10.61784/wjer3120

MULTI-OBJECTIVE OPTIMIZATION AND ROBUST SCREENING MODELING OF AQUEOUS ELECTROLYTE FORMULATIONS

PengYuan Zhang, EnCi Zhang, HaoShan Sun, FengShuo Liu, DanZhi Wang*
Century College, Beijing University of Posts and Telecommunications, Beijing 102101, China.
**Corresponding Author: DanZhi Wang*

Abstract: Aqueous electrolyte formulation optimization involves coupled conductivity, acid-base compatibility, electrochemical stability, and preparation robustness under limited experimental budgets. Based on 251 experimental records, this study constructs an integrated modeling framework for performance evaluation, predictive modeling, mechanism interpretation, reliability assessment, and candidate formulation screening. The original stock-solution volumes, molalities, densities, component existence indicators, ionic load, mass load, Li/Na ratio, anion-family proportions, water volume fraction, and component entropy are organized into a unified feature space. Conductivity, pH, and the electrochemical stability window measured at the 1 mA/cm2 threshold are then combined with robustness indicators to support multi-objective formulation ranking. Ridge regression, random forest, and Gaussian process regression are compared under random and structural validation. The Gaussian process model performs best for conductivity prediction, while random forest provides the strongest pH and stability-window predictions. Feature importance and response analysis show that total ion load dominates conductivity, Li/Na-related descriptors influence pH, and NaBr-related descriptors strongly affect the electrochemical window. Candidate formulations are further screened through Bayesian optimization and local perturbation analysis, identifying NaClO4-NaNO3 systems as high-potential and robust candidates for subsequent experiments.
Keywords: Aqueous electrolyte; Formulation optimization; Random forest; Gaussian process regression; Robustness analysis

1 INTRODUCTION

Aqueous electrolytes have become an important direction in electrochemical energy-storage research because they offer intrinsic safety, low cost, high ionic conductivity, and environmental compatibility compared with many organic electrolyte systems. However, practical aqueous formulations are not determined by a single salt concentration. Their conductivity, acid-base compatibility, electrochemical stability window, and preparation tolerance are jointly controlled by coupled ion species, water proportion, anion families, and concentration ratios. This coupling makes formulation design a typical multi-factor and multi-objective optimization problem rather than a simple empirical screening task [1-3].

Previous electrolyte studies have provided two main lines of methodological support. Experimental studies have clarified that mixed salts and additives can widen the operating window and improve compatibility, but exhaustive trial-and-error experiments are expensive when the component space expands. Data-driven studies have introduced regression models, random forest, Gaussian process regression, Bayesian optimization, and automated experimentation to accelerate electrolyte discovery [4-6]. At the experimental level, recent work has emphasized highly concentrated and hybrid aqueous electrolytes, interfacial stabilization, and composition-dependent transport behavior. At the methodological level, automated laboratories and uncertainty-aware optimization have begun to replace exhaustive enumeration. Nevertheless, many published workflows still evaluate formulations within randomly divided samples and rarely combine cross-family validation, local confidence, and tolerance to preparation errors in a unified decision process for engineering recommendation tasks. These studies show the value of machine learning for battery-material design, yet several limitations remain: random validation may overestimate cross-family generalization, a conductivity-only target may ignore pH and stability constraints, and high-scoring points may be fragile if small preparation deviations sharply reduce performance [7-9].

Based on these research gaps, this paper treats aqueous electrolyte design as a joint problem of performance prediction, reliability assessment, and robust candidate screening. The dataset contains 251 experimental records involving Li2SO4, LiClO4, LiNO3, Na2SO4, NaBr, NaClO4, NaNO3, and water, with conductivity, pH, and the 1 mA/cm2 electrochemical stability window as the main responses. Because the samples cover different formulation families and density regions, the modeling process must distinguish trustworthy interior regions from sparse boundary regions while still allowing promising unexplored candidates to be selected.

The logical structure of this study is therefore arranged as follows. First, original stock-solution volumes and derived chemical descriptors are organized into a unified feature space, and conductivity, pH suitability, electrochemical stability, and local robustness are combined into a performance-evaluation system. Second, Ridge regression, random forest, and Gaussian process regression are compared under both random and structural validation to evaluate prediction

ability and generalization risk. Third, feature importance and response analysis are used to interpret the roles of ionic load, Li/Na ratio, and NaBr-related descriptors. Finally, Bayesian candidate selection and local perturbation analysis are integrated to recommend high-potential, robust NaClO4-NaNO3 formulations for subsequent closed-loop experiments [10].

2 PERFORMANCE EVALUATION SYSTEM

2.1 Indicator Design

The performance-evaluation system contains conductivity, pH friendliness, electrochemical stability, and local robustness. Conductivity reflects ion-transport efficiency and is normalized to enable comparison with other indicators. pH friendliness measures the distance from the desired mild chemical environment. The electrochemical stability window is calculated from the difference between anodic and cathodic limits under the 1 mA/cm^2 criterion. These indicators are used together because none of them alone can represent the full application value of an aqueous electrolyte.

$$S=w_1z_\sigma+w_2z_{pH}+w_3z_{EW},\ w_1+w_2+w_3=1 \tag{1}$$

Equation (1) follows the original weighted comprehensive-performance expression, where z_sigma, zpH, and zEW denote the standardized conductivity, pH suitability, and electrochemical-window indicators, and the three weights sum to one.

$$R=\lambda_1R_1+\lambda_2R_2+\lambda_3R_3 \tag{2}$$

Equation (2) follows the original stability aggregation expression, where R1, R2, and R3 denote stability-related sub-indicators and lambda1, lambda2, and lambda3 are their weights.

$$\mathrm{MAE}=\frac{1}{n}\sum_{i=1}^{n}\mid y_i-\hat{y}_i\mid \tag{3}$$

$$\mathrm{RMSE}=\sqrt{\frac{1}{n}\sum_{i=1}^{n}(y_i-\hat{y}_i)^2} \tag{4}$$

Model performance is evaluated with the original MAE, RMSE, and R2 definitions. These metrics respectively describe average absolute error, root mean square error, and goodness of fit, so they are used together to compare Ridge, Random Forest, and GPR predictions.

$$R^2=1-\frac{\sum_{i=1}^{n}(y_i-\hat{y}_i)^2}{\sum_{i=1}^{n}(y_i-\bar{y})^2} \tag{5}$$

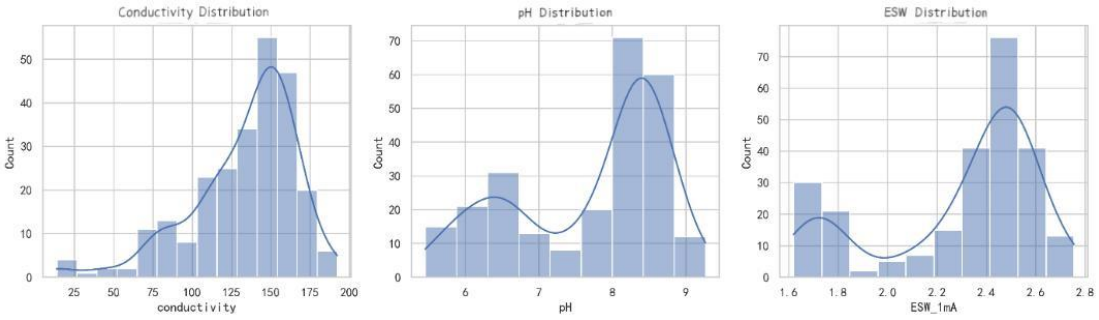

Figure 1 Distribution of Target Performance Indicators

Figure 1 shows that conductivity is close to a unimodal distribution concentrated around 100-175 mS/cm. The pH distribution is clearly bimodal, with samples concentrated in weakly acidic and weakly alkaline intervals. The electrochemical stability window also exhibits two value regions, indicating that the formulation space has distinct stability layers. These distributional characteristics support later stratification, reliability analysis, and candidate selection.

2.2 Feature Construction

Each experimental record is transformed from sparse formulation dictionaries into a fixed-dimensional feature vector. The original volume of each component is retained, and missing components are filled with zero. Existence indicators are added to distinguish absent salts from low-volume salts. Derived descriptors include total ionic load, total mass load, Li total volume, Na total volume, nitrate total volume, perchlorate total volume, sulfate total volume, Li/Na ratio, sulfate/nitrate ratio, non-water component count, water volume fraction, and component entropy.

$$C(x)=\alpha_1\bar{\rho}(x)+\alpha_2(1-\bar{u}(x))+\alpha_3(1-\bar{e}_{loc}(x)) \tag{6}$$

Equation (6) follows the original model-confidence expression, where the normalized density, uncertainty, and local error jointly determine whether a candidate is located in a trustworthy region. The source statistics show that volume-

weighted total ionic load changes from 0.43 to 16.03 and has a conductivity correlation of about 0.406; estimated total mass ranges from 7.135 to 11.620 and correlates with conductivity at about 0.359. The symbol definitions used in subsequent modeling and candidate screening are summarized in Table 1.

Table 1 Symbol Description

Symbol	Meaning
x	Formulation feature vector
C	Conductivity
pH	pH value
EW	Electrochemical window indicator
S	Comprehensive performance score
R	Robustness score
y_hat	Predicted value
e	Prediction error
sigma	Prediction uncertainty
rho	Local sample density
T	Trustworthiness score
A	Candidate acquisition score

3 PREDICTIVE MODELING AND VALIDATION

3.1 Model Construction

The formulation-performance relationship contains linear trends, nonlinear interactions, and local uncertainty. Ridge regression is used as a linear baseline because it can reveal stable main effects under limited samples. Random forest is used to capture nonlinear component interactions and is less sensitive to monotonic transformations of features. Gaussian process regression is used because it provides both a predicted mean and prediction uncertainty, which are important for active candidate selection [5].

The input features are standardized after median imputation. Conductivity, pH, and the 1 mA/cm^2 electrochemical stability window are treated as the three main output targets. Small explicit interaction terms, such as salt concentration multiplied by water proportion or Li/Na ratio multiplied by total ionic load, are only used in the linear baseline to retain interpretability. For tree-based and probabilistic models, nonlinear interactions are mainly learned from the data [6].

Table 2 Random and Structural Validation Performance of Three Predictive Models

Target	Metric	Ridge	Random Forest	GPR
Conductivity	MAE	12.7264 / 24.0738	7.5147 / 8.4121	8.0598 / 12.0962
Conductivity	RMSE	20.6451 / 32.0816	19.0690 / 19.4678	18.4588 / 21.8056
Conductivity	R^2	0.6269 / 0.0990	0.6817 / 0.6682	0.7017 / 0.5838
pH	MAE	0.3476 / 1.0211	0.1662 / 0.3498	0.2011 / 0.4886
pH	RMSE	0.4637 / 1.2370	0.2918 / 0.5586	0.3322 / 0.6578
pH	R^2	0.8008 / -0.4176	0.9211 / 0.7110	0.8977 / 0.5991
1 mA/cm^2 EW	MAE	0.0554 / 0.1069	0.0432 / 0.0665	0.0452 / 0.0734
1 mA/cm^2 EW	RMSE	0.0768 / 0.1315	0.0633 / 0.1127	0.0659 / 0.0983
1 mA/cm^2 EW	R^2	0.9440 / 0.8357	0.9619 / 0.8793	0.9588 / 0.9082

Table 2 reports the paired random-validation and structural-validation results. Gaussian process regression gives the best conductivity RMSE in random validation, while random forest gives the strongest pH and electrochemical-window performance. The structural validation results are generally weaker than random validation, which means that random splitting can overestimate cross-family generalization when nearby formulations appear in both training and test sets [7].

3.2 Feature Importance and Response Interpretation

Model interpretation indicates that total ionic load is the dominant conductivity descriptor, with an importance of 0.3961. Component entropy, Li_2SO_4-related load, Li_2SO_4 volume, total mass, and NaBr-related variables provide additional conductivity information. For pH prediction, Li/Na ratio and Li total volume are the leading variables, with importances of 0.3660 and 0.3470. For the electrochemical window, NaBr presence is the most influential factor, with an importance of 0.2496, and NaBr-related load also has a strong contribution.

Figure 2 and Figure 3 show that the same descriptor may have different effects on different targets. A higher ionic load initially improves conductivity, but the response tends to flatten or decline after a high-load interval. Li-related descriptors mainly affect the pH response, while NaBr-related descriptors show a negative or threshold-like influence on the electrochemical window. These patterns support the need for multi-objective balancing rather than unidirectional maximization.

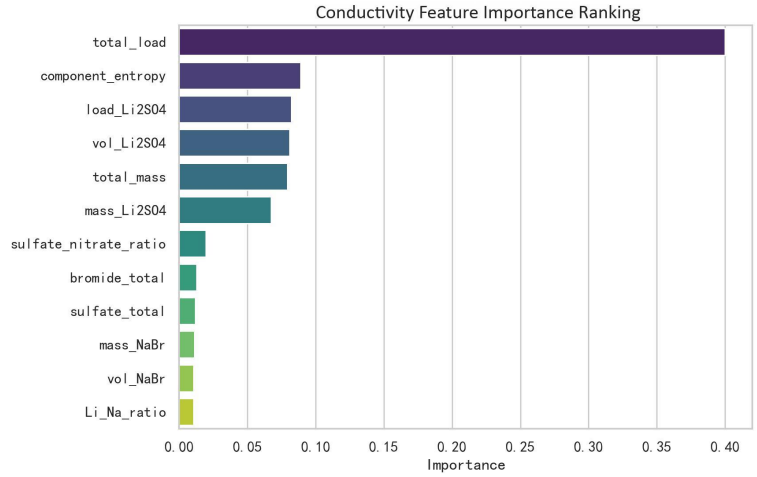

Figure 2 Feature-Importance Ranking for Conductivity Prediction

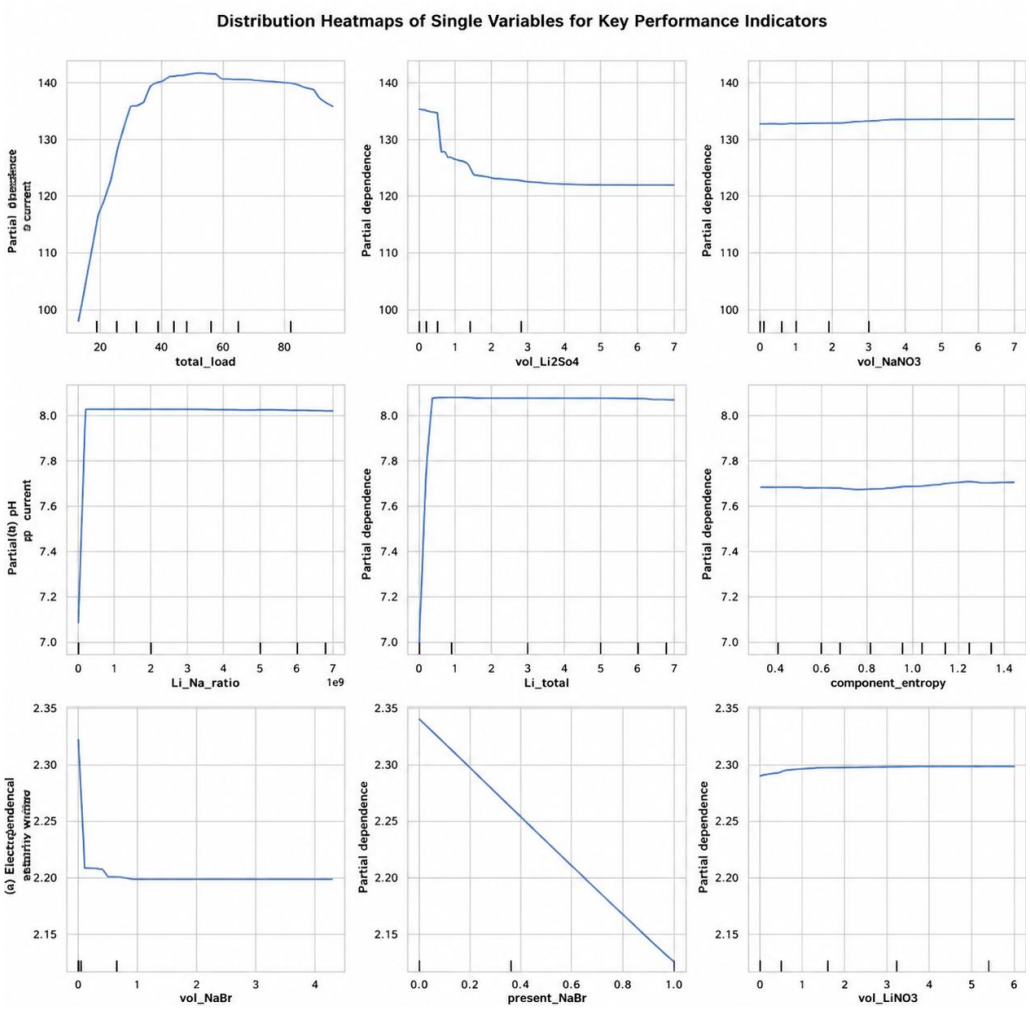

Figure 3 Partial-Dependence Responses of Key Performance Indicators

4 RELIABILITY ANALYSIS AND CANDIDATE DESIGN

4.1 Trustworthy Region Identification

Prediction accuracy is not the same as usability. The source formulation space has obvious clustering and uneven density, so a model may be reliable in dense interior regions but unstable near sparse boundaries. The reliability score combines local density, prediction uncertainty, and local historical error. A high score means that the surrounding samples are sufficient, the model uncertainty is low, and the local error is limited [8].

$$\mathrm{EI}(x)=E[\max(0,f(x)-f(x^{*}))] \tag{7}$$

Equation (7) is the original expected-improvement acquisition function. It gives candidate points with high predicted improvement a larger sampling priority, while still allowing sparse promising regions to be explored.

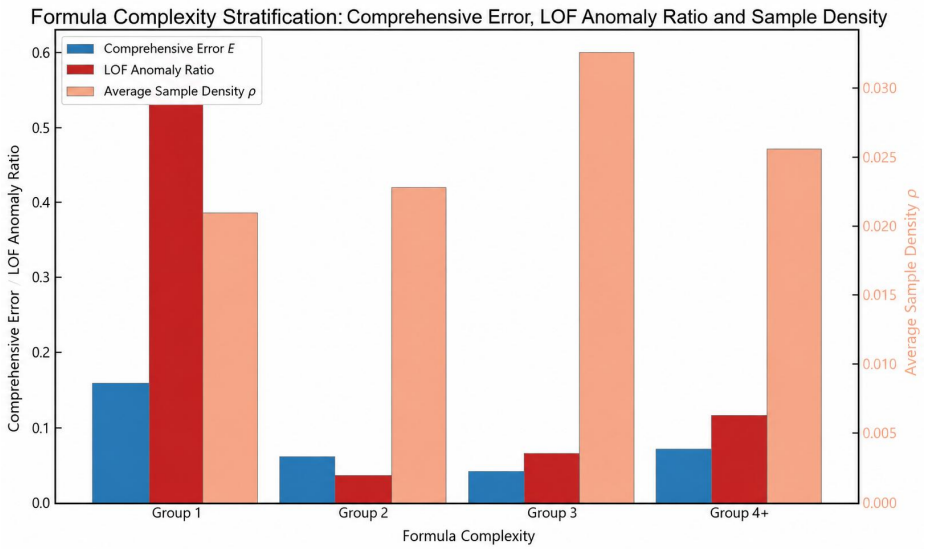

Figure 4 Formulation Complexity, Integrated Error, Anomaly Ratio, and Sample Density

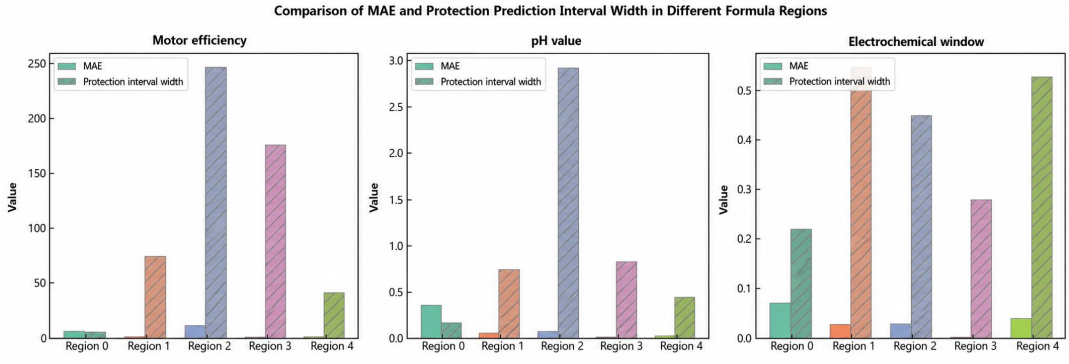

Figure 5 Regional Error and Conservative Prediction Interval Comparison

Figure 4 indicates that single-component formulations have a high anomaly proportion and low sample density, whereas three-component formulations show the lowest integrated error and the highest density. Figure 5 further demonstrates that different clusters have heterogeneous error levels. The high-confidence core region is the area where density is high and regional error is low; low-density and high-error clusters should be used mainly for exploratory sampling rather than direct engineering recommendation.

4.2 Bayesian Candidate Selection

Candidate formulation design balances exploitation and exploration. Exploitation favors high predicted performance, while exploration favors informative samples with larger uncertainty. Gaussian process regression provides the predicted mean and uncertainty needed for acquisition functions. For a small batch of additional experiments, the source strategy uses a mixed configuration: development-type samples verify promising regions, while exploration-type samples supplement sparse or boundary regions [9].

$$\max f_1(x)=\text{Conductivity} \tag{8}$$

Equations (8)-(10) follow the original Pareto-objective setting. Conductivity is maximized, the deviation from the target pH is minimized, and robustness is maximized. Candidate filtering is therefore not based only on a single score; it also requires pH compatibility, trustworthiness, and distance from existing samples.

5 ROBUST SCREENING OF CANDIDATE FORMULATIONS

5.1 Local Perturbation Analysis

Robustness is defined as the ability of a formulation to maintain high comprehensive performance when component proportions are slightly perturbed. Each candidate is evaluated by local Monte Carlo perturbation, where non-water components are changed within a small range and water is redistributed to keep total volume approximately constant.

The random forest model predicts conductivity, pH, and the stability window for perturbed samples, and the comprehensive score is recalculated.

Three indicators are used: average sensitivity, worst decline, and local standard deviation. Average sensitivity measures the mean performance loss in the neighborhood; worst decline measures the largest observed deterioration; local standard deviation measures volatility. A candidate is treated as fragile when the worst decline exceeds 10% of the base score. This design distinguishes high-performance plateaus from isolated sharp peaks.

$$\min f_2(x) = \left| \mathrm{pH}(x) - \mathrm{pH}^* \right| \tag{9}$$

The local perturbation indicators are interpreted according to the original definitions of average variation, worst decline, local standard deviation, and plateau robustness. These indicators distinguish flat high-performance regions from isolated performance peaks.

$$\max f_3(x) = R(x) \tag{10}$$

Table 3 Robustness Comparison of Representative Candidate Formulations

Candidate formulation	Base score	Local std.	Worst decline	Robustness judgment
$NaClO_4$=1.0, $NaNO_3$=5.0, water=1.0	0.8666	0.0019	0.0085	Robust plateau
$NaClO_4$=2.0, $NaNO_3$=3.0, water=2.0	High score	0.0009	Low	Very stable candidate
$NaClO_4$=1.0, $NaNO_3$=6.0	0.8659	0.0227	0.1366	Fragile high-score peak
Na_2SO_4=0.6, $NaClO_4$=4.6, water=1.8	0.8458	0.0094	0.0239	Balanced backup candidate
$NaClO_4$=2.0, $NaNO_3$=5.0	High score	0.0024	Low	Robust candidate
$NaClO_4$=1.0, $NaNO_3$=3.0, water=3.0	High score	0.0011	Low	Robust candidate

Table 3 shows that $NaClO_4$-$NaNO_3$ formulations are the most valuable recommendation family. The formulation $NaClO_4$=1.0, $NaNO_3$=5.0, water=1.0 has a comprehensive score of 0.8666, a local standard deviation of only 0.0019, an average decline of 0.0007, and a worst decline of 0.0085, with a plateau robustness value of 539.5239. By contrast, $NaClO_4$=1.0, $NaNO_3$=6.0 has a high base score and a predicted stability window of 2.5686 V, but its local standard deviation reaches 0.0227 and the worst decline reaches 0.1366, showing that it is closer to a fragile isolated peak.

5.2 Final Recommendation

The final screening divides candidates into three groups. The priority robust-plateau group includes $NaClO_4$=1.0, $NaNO_3$=5.0, water=1.0; $NaClO_4$=2.0, $NaNO_3$=3.0, water=2.0; $NaClO_4$=2.0, $NaNO_3$=5.0; and $NaClO_4$=1.0, $NaNO_3$=3.0, water=3.0. These candidates combine high predicted performance with very low local volatility and are suitable for the next development experiments.

The balanced backup group includes Na_2SO_4=0.6, $NaClO_4$=4.6, water=1.8 and $NaClO_4$=1.0, $NaNO_3$=4.0, water=2.0. Their performance is high and robustness is generally acceptable, but their local volatility is slightly higher than that of the best plateau candidates. The fragile high-score group includes $NaClO_4$=1.0, $NaNO_3$=6.0. Although its static prediction is attractive, perturbation analysis shows a clear amplification risk, so it should not be used as the first scale-up formulation without additional verification.

6 MODEL EVALUATION AND IMPROVEMENT

The proposed framework has several advantages. It links performance evaluation, predictive modeling, reliability analysis, active design, and robust screening into one workflow. It avoids the limitations of single-index conductivity ranking and incorporates pH, electrochemical stability, and perturbation tolerance. Random forest provides strong nonlinear prediction for pH and the stability window, Gaussian process regression supplies useful uncertainty for experimental design, and Ridge regression gives interpretable linear baselines. SHAP-style importance, partial dependence, and interaction responses also help explain the role of key components.

The framework still has limitations. If electrochemical curves provide only summary values, dynamic features such as peak position, peak area, turning-point slope, and plateau length cannot be fully used. Physicochemical descriptors such as ionic radius, solvation characteristics, solubility, viscosity, and dielectric information remain incomplete. Local perturbation robustness is also a model-based approximation, while real experiments may include temperature variation, mixing sequence, measurement noise, and environmental disturbances. Future work should add richer curve descriptors, conformal prediction or quantile regression, and rolling updates from new experiments so that confidence estimation becomes more reliable in sparse regions.

After each new experiment, the result can be added back to the training set, and the predictive model, trustworthiness score, acquisition score, and robustness score can be updated together. This rolling update reduces the mismatch risk of static modeling and gradually improves generalization to under-sampled formulation regions. Therefore, the recommended workflow is not a one-time ranking list, but a prediction-experiment-update cycle that continuously refines the aqueous electrolyte design space.

The closed-loop feedback mechanism is also important. Newly selected experiments should be divided into development-type and exploration-type samples. Development-type samples verify whether high-scoring candidates are experimentally achievable, while exploration-type samples supplement low-density, high-uncertainty, or boundary regions. Candidates with high uncertainty, low trustworthiness, and high perturbation risk should be treated as warning samples for boundary correction rather than as immediate scale-up targets.

The high-potential samples in the original data are mainly concentrated in $NaNO_3$ single-salt systems and $NaClO_4$-$NaNO_3$ double-salt systems. For example, the $NaNO_3$=7.0 single-salt system has a conductivity of 173.4 mS/cm, pH of 6.17, and electrochemical stability window of 2.6121 V. The $NaClO_4$=1.0, $NaNO_3$=5.0, water=1.0 system has a conductivity of 170.5 mS/cm, pH of 7.54, and stability window of 2.5464 V. The $NaClO_4$=1.0, $NaNO_3$=6.0 system has a conductivity of 165.7 mS/cm, pH of 7.62, and stability window of 2.5799 V. These values show why the $NaClO_4$-$NaNO_3$ region is repeatedly selected by the optimization model.

Family-level statistics further support the candidate-screening logic. The Na_2SO_4-NaBr-$NaClO_4$-$NaNO_3$ family has the highest average conductivity, reaching 160.8189 mS/cm, but its average pH is only 6.3259 and its average 1 mA/cm^2 electrochemical stability window is only 1.7356 V. This means that high conductivity alone may be accompanied by weaker acid-base compatibility and a narrower stable voltage interval. In contrast, the $NaClO_4$-$NaNO_3$ family has an average conductivity of 148.4778 mS/cm, an average pH of 7.6456, and an average stability window of 2.5131 V, so it is more balanced across the three core targets.

7 FAMILY-LEVEL EVIDENCE AND CLOSED-LOOP DESIGN

The three-objective candidate distribution illustrates the different functions of development-type and exploration-type samples. Development-type points are concentrated around high-performance and high-trust regions, so they are suitable for direct validation. Exploration-type points extend toward sparse regions and potential boundaries, which helps the model correct uncertainty and discover new formulation opportunities. This division is consistent with the source strategy of using a mixed experimental batch rather than relying on random selection.

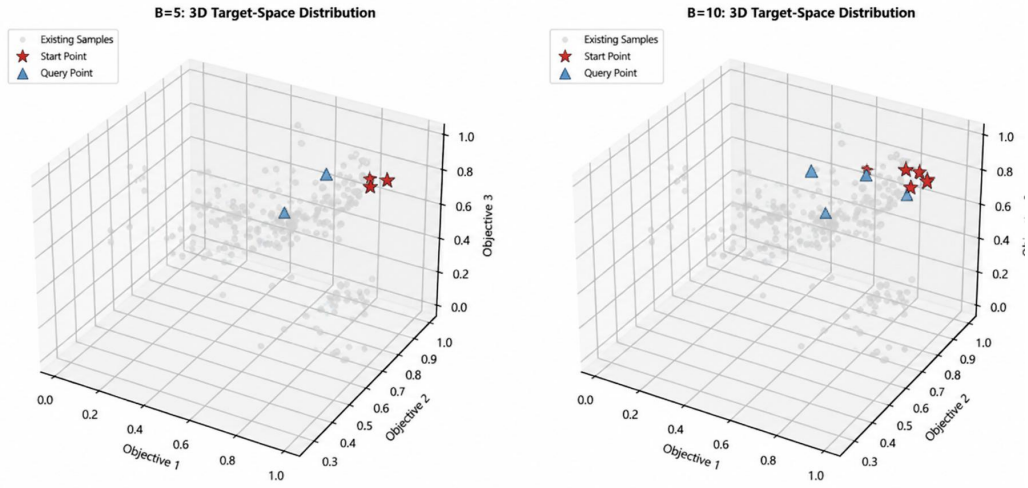

Figure 6 Candidate Distribution in Three-Objective Space

8 CONCLUSION

This study constructs an integrated data-driven framework for aqueous electrolyte formulation optimization using the 251-record experimental set. The analysis shows that a good formulation should not be selected by conductivity alone, because pH compatibility, electrochemical stability, model trustworthiness, and local robustness are equally important. The predictive results indicate that Gaussian process regression is most competitive for conductivity prediction, while random forest is strongest for pH and electrochemical-window prediction. Interpretation results identify total ionic load, Li/Na-related descriptors, Li total volume, and NaBr-related descriptors as key factors governing different targets [10].

The candidate design strategy balances exploitation and exploration through model mean, uncertainty, density, and pH constraints. Robustness screening further distinguishes stable high-performance plateaus from fragile single-point peaks. The $NaClO_4$-$NaNO_3$ family, especially $NaClO_4$=1.0, $NaNO_3$=5.0, water=1.0 and $NaClO_4$=2.0, $NaNO_3$=3.0, water=2.0, shows strong engineering potential because it combines high predicted performance with low local perturbation sensitivity. The framework can support subsequent closed-loop experimentation by updating models after new validation results are obtained.

Several limitations should also be considered. First, the 251-record dataset is still limited for fully describing sparse or boundary formulation regions, so predictions near low-density areas may have higher uncertainty. Second, the current model mainly uses formulation-level descriptors and summary electrochemical indicators; richer curve features, viscosity, ion solvation descriptors, temperature sensitivity, and repeated-experiment noise should be incorporated in future studies. Third, the robustness analysis is model-based and should be verified through additional perturbation experiments before scale-up. Future work should therefore follow a closed-loop route in which new experimental results are continuously added to update the predictive model, trustworthiness score, acquisition strategy, and robust-screening rules.

COMPETING INTERESTS

The authors declare that they have no competing interests.

REFERENCES

[1] Ji D, Kim J. Trend of developing aqueous liquid and gel electrolytes for sustainable, safe, and high-performance Li -ion batteries. Nano-Micro Letters, 2024, 16(1): 2.
[2] Xu J J, Ji X, Zhang J X, et al. Aqueous electrolyte design for super-stable 2.5 V LiMn2O4||Li4Ti5O12 pouch cells. Nature Energy, 2022, 7(2): 186-193.
[3] Xu G S, Jiang M X, Li J L, et al. Machine learning-accelerated discovery and design of electrode materials and electrolytes for lithium ion batteries. Energy Storage Materials, 2024, 72: 103710.
[4] Yik J T, Hvarfner C, Sjolund J, et al. Accelerating aqueous electrolyte design with automated full-cell battery experimentation and Bayesian optimization. Cell Reports Physical Science, 2025, 6(5): 102548.
[5] Dave A, Mitchell J, Burke S, et al. Autonomous optimization of non-aqueous Li-ion battery electrolytes via robotic experimentation and machine learning coupling. Nature Communications, 2022, 13: 5454.
[6] Xu G S, Zhang Y J, Jiang M X, et al. A machine learning-assisted study on organic solvents in electrolytes for expanding the electrochemical stable window of zinc-ion batteries. Chemical Engineering Journal, 2023, 476: 146676.
[7] Huang G C, Huang F Q, Dong W J. Machine learning in energy storage material discovery and performance prediction. Chemical Engineering Journal, 2024, 492: 152294.
[8] Wang Y. Application-oriented design of machine learning paradigms for battery science. NPJ Computational Materials, 2025, 11: 89.
[9] Wang F, Tang Y H, Ma Z B, et al. Domain oriented universal machine learning potential enables fast exploration of chemical space of battery electrolytes. Nature Communications, 2026, 17: 1226.
[10] Nguyen T M, Biressaw G M, Lee M H, et al. Hybrid aqueous electrolyte design for interfacial stabilization in high -energy-density and long-life LiNi0.8Mn0.1Co0.1O2-Li4Ti5O12 lithium-ion batteries. Journal of Energy Storage, 2025, 139: 118915.